Cardiac Memory in Human Atria and Relation to Arrhythmogenesis

C Sánchez[1,2], E Pueyo[1,2,3], P Laguna[1,2], B Rodríguez[3]

[1]Instituto de Investigación en Ingeniería de Aragón (I3A), Universidad de Zaragoza, Spain
[2]CIBER de Bioingeniería, Biomateriales y Nanomedicina (CIBER-BBN), Spain
[3]Computing Laboratory, University of Oxford, UK

Abstract

Abnormal adaptation of action potential duration (APD) to changes in heart rate (HR) has been suggested as an indicator of increased arrhythmic risk. In this study, we investigate the mechanisms underlying APD rate adaptation in human atrial cells and its relationship to arrhythmogenesis. Simulations are performed using action potential computational models and results are compared with experimental data from the literature. APD rate adaptation in response to sudden sustained HR changes is shown to take more than 8 minutes to be completed in the simulations and two main adaptation phases can be identified: a fast initial one due to the Na^+/Ca^{2+} exchanger and the L-type calcium current; and a subsequent slow accommodation determined by intracellular Na dynamics. Both APD adaptation dynamics and its underlying mechanisms are found to be consistent in different species. Alterations in ionic mechanisms leading to delayed APD adaptation are associated with increased proarrhythmic risk.

1. Introduction

Cardiac arrhythmias, defined as conditions involving abnormalities in heart rhythm, represent a serious health problem in industrialized countries. Among cardiac arrhythmias, those generated in the atria, despite being considered less dangerous than ventricular ones, are much more commonly diagnosed. A large body of research has been devoted to the study of atrial arrhythmias in the last several decades, but, nevertheless, the mechanisms leading to their genesis and maintenance remain rather elusive. It is known that after a sudden sustained change in heart rate (HR), the electrophysiology of atrial cells is altered, which leads to observable changes in action potential (AP). Some experimental studies have suggested that impaired adaptation of AP duration (APD) to HR changes is associated with an increased likelihood for the development of arrhythmias [1].

Short-term cardiac memory (CM), which determines APD rate adaptation, has been studied in human ventricular cells [2] as well as in atrial cells of other species [1]. However, there is very limited knowledge of short-term CM in human atria. In this study, we use a detailed mathematical model of human atrial AP [3] to investigate the mechanisms underlying CM in human atria and its relationship to arrhythmogenesis. Interspecies as well as atrial-ventricular comparisons are performed to fully characterize the nature of APD rate adaptation in cardiac mammalian cells.

The main objectives of our study can be summarized as follows: 1) characterize short-term CM in human atrial cardiomyocytes; 2) elucidate the ionic mechanisms underlying CM; 3) evaluate the relationship between atrial APD rate adaptation and proarrhythmic risk; 4) assess short-term CM in human hearts.

2. Methods

2.1. Cell model

The human atrial cell model developed by Courtemanche *et al* [3] is used for AP simulation. A 2-ms square stimulus pulse of strength 2 nA (twice diastolic threshold) is applied to individual cells. The forward Euler method with a time step $\Delta t = 0.02$ ms is used to compute membrane potential (V) according to (1): $dV/dt=-(I_{ion}+I_{st})/C_m$, where I_{ion} is the sum of all ionic currents across the membrane, I_{st} is the stimulus current, and C_m is the total membrane capacitance. The same method is applied to integrate and derive the ionic concentrations and gating variables of all the ionic currents in the model. APD denotes AP duration measured at 90% repolarization.

2.2. APD rate adaptation and underlying mechanisms

APD rate adaptation is evaluated using the following pacing protocol: cycle length (CL) is stepwise changed after 10 minutes of stimulation from 1000 ms to 600 ms, maintained for 10 minutes and changed back to 1000 ms for other 10 minutes. The time required for APD to

complete 90% of the difference between its initial and final steady-state values at each stage is denoted by t_{90}.

Two different phases, fast and slow, of APD adaptation following HR changes are identified. Each of those phases is fitted with a four-parameter exponential function of the form (2): $f(t)=a+be^{-(t-c)/\tau}$. Time constants, τ_{fast} and τ_{slow}, derived from equation (2) are used to characterize fast and slow phases, respectively.

To elucidate the ionic mechanisms underlying APD rate adaptation, the conductances and time constants of gating variables associated with all the ionic currents are varied between -30% and +30% of their default values.

2.3. Proarrhythmic risk markers

1) *Restitution slopes*: S1-S2 and dynamic restitution slopes have been related to arrhythmic risk [4]. For the S1-S2 protocol, 10 S1 stimuli are applied every 1000 ms followed by an S2 extra-stimulus applied at varying diastolic interval (DI) after the last generated AP. The APD restitution (APDR) curve is obtained by plotting the APD calculated for the S2 stimulus versus the preceding DI. For the dynamic protocol, a series of 100 stimuli at an initial CL=3000 ms is applied. The CL is subsequently decreased and the APDR curve is obtained by plotting the last APD of each series versus the last DI [5].

To compute S1-S2 and dynamic APDR slopes, the restitution curves are fitted with functions of the form (3): $APD=a(1-e^{-bDI})+c$, in the range of DIs between 0 and 400 ms. S_{S1S2} and S_{dyn} (APDR slopes) are calculated by evaluating the derivative of (3) at a DI of 100 ms.

2) *Calcium current reactivation*: the degree of recovery from inactivation of the L-type calcium current (I_{CaL}) has been suggested as an indicator of the likelihood of arrhythmia generation [6]. In this study, we compute the product of f (voltage-dependent I_{CaL} inactivation gate) and f_{Ca} (calcium-dependent inactivation I_{CaL} gate) at 90% repolarization of steady-state AP at a CL of 1000 ms, and we denote it by ρ. Values of ρ close to "1" are indicative of high probability of calcium current reactivation.

3) *AP triangulation*: a close relationship between AP triangulation and proarrhythmia has been shown in [7]. In order to describe the AP shape, the ratio between APD_{90} and APD_{50} (APD measured at 90% and 50% repolarization, respectively) is computed for steady-state AP at a CL of 1000 ms, and it is denoted by δ. Large values of δ (>>1) correspond to triangular APs.

3. Results

3.1. Characterization of cardiac memory

Figure 1 shows time courses of APD adaptation after HR deceleration and acceleration obtained from simulations and from experiments in canine atrial tissue using the same stimulation protocol described in [1]. Due to the unavailability of experimental data from human, the comparison is performed using data from dog, which shows great similarity in repolarization properties. In both, a sudden sustained HR change induces an initial large variation in APD, which is followed by a slower accommodation at the end of which APD reaches its new steady-state value.

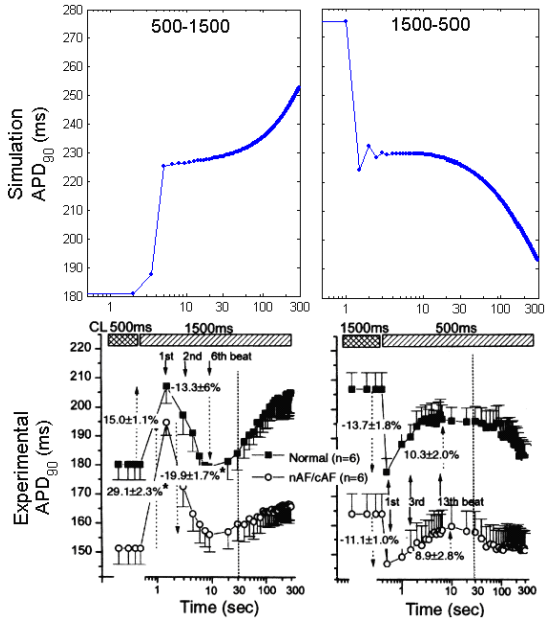

Figure 1. Simulation vs. experimental (modified from [1]) APD rate adaptation.

Using the pacing protocol described in section 2 (CL: 1000-600-1000 ms), the time t_{90} required in the simulations for APD to complete its rate adaptation is found to be 487 s after HR acceleration, and 564 s after HR deceleration.

The fast initial APD adaptation, which occurs in the first 1-5 beats after the CL change, is characterized by a time constant τ_{fast} that takes values of 6.4 s following HR acceleration and 7.3 s following HR deceleration. The second slow phase, which lasts for some minutes, is characterized by a time constant τ_{slow} of 297.2 s after HR acceleration and 404.3 s after HR deceleration.

A sensitivity analysis is performed to assess the dependence of APD adaptation characteristics on the initial CL and the magnitude of CL change. Figure 2 shows that both τ_{fast} and τ_{slow} are significantly dependent on the initial CL (analysis of variance, $p<0.05$), with τ_{fast} gradually decreasing from >100 s when the initial CL=2000 ms to <8 s when the initial CL=1000 ms; and τ_{slow} gradually increasing from ~240 s for CL=2000 ms to >300 s for CL=1000 ms. Regarding the magnitude of CL change, τ_{slow} is not clearly dependent on that magnitude, while τ_{fast} slightly varies from >12 s to <5 s when the CL magnitude change is varied from 200 to 600 ms.

	HRacceleration		HRdeceleration	
	τ_{fast}(s)	τ_{slow}(s)	τ_{fast}(s)	τ_{slow}(s)
1000-600-1000	6.4	297.2	7.3	404.3
1600-1200-1600	58.8	239.8	33.4	274.1
2000-1600-2000	176.2	231.0	99.4	240.3
1000-800-1000	23.2	190.6	12.0	449.6
1000-400-1000	1.6	245.2	4.4	593.2

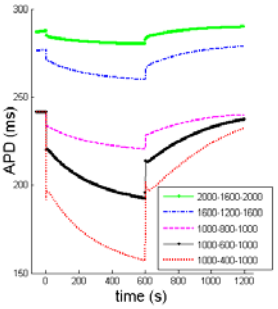

Figure 2. Simulated APD time courses under different CL changes.

3.2. Ionic mechanisms of rate adaptation

To elucidate the ionic mechanisms underlying the fast phase of APD rate adaptation, τ_{fast} values are computed after varying all the conductances and gating properties of ionic currents in the model. Conditions involving maximal conductances of I_{CaL} and the Na^+/Ca^{2+} exchanger (G_{CaL} and G_{NaCa}, respectively) are the ones leading to the greatest alterations in τ_{fast} values. To confirm this finding, Figure 3 (top row) shows that large degrees of inhibition of I_{CaL} and/or the Na^+/Ca^{2+} exchanger lead to abolishment of the fast adaptation phase. A quantification of this fact is presented in the upper row of Figure 4, which shows that 30% reduction of G_{CaL} or G_{NaCa} cause a substantial increase in τ_{fast} values (τ_{fast}=7.5, 9.2 s under 30% reduction of G_{CaL} and G_{NaCa}, respectively, whereas the value in control conditions is 6.4 s, following HR acceleration; τ_{fast} values are 12.1, 10.1 and 7.3 s, respectively, following HR deceleration).

Regarding the slow phase of APD adaptation, we show that this is closely related to $[Na^+]_i$ dynamics. Figure 3 (bottom row) shows that clamping $[Na^+]_i$ to its steady-state value (14.9 mM for CL=600 ms, and 14.0 mM for CL=1000 ms) leads to abolishment of the slow phase.

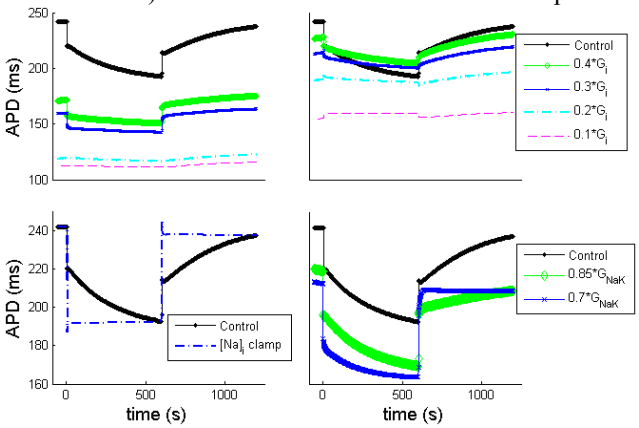

Figure 3. APD time course under control, G_{CaL} inhibition (denoted by G_i, left-top panel), G_{NaCa} inhibition (denoted by G_i, right-top panel), $[Na^+]_i$ clamping (left-bottom panel), and G_{NaK} inhibition (right-bottom panel).

Inhibition of the Na^+/K^+ pump has notable effects on $[Na^+]_i$ dynamics and, consequently, on τ_{slow}, as shown in the second row of Figure 4 (τ_{slow}=601.9 s under 30% Na^+/K^+ pump inhibition, while control value is 297.2 s, after HR acceleration; τ_{slow}=780.1 s and 404.3 s, respectively, after HR deceleration).

With the aim of confirming that our observations are model independent, the same simulations described above are performed using the model developed by Nygren et al [8]. The ionic mechanisms involved in the fast and slow phase of APD rate adaptation are found to be the same using either of the two models.

3.3. Atrium-ventricle comparison

Analogies and differences in CM between atria and ventricles are investigated by comparing the results from the present study with those reported in [2] for human ventricular cells. Although atrial and ventricular APs are substantially different in shape and duration, APD is found to adapt in a similar way in the two cases, with both fast and slow phases characterizing their adaptation dynamics. Ionic mechanisms underlying the fast initial adaptation phase are somewhat different, with the key players being the kinetics of I_{CaL} and I_{Ks} (slow delayed rectifier potassium current) in the ventricle [2], and maximal conductances G_{NaCa} and G_{CaL} in the atrium. However, ionic mechanisms underlying the slow phase of APD rate adaptation are common to atria and ventricles, and are mainly determined by $[Na^+]_i$ dynamics.

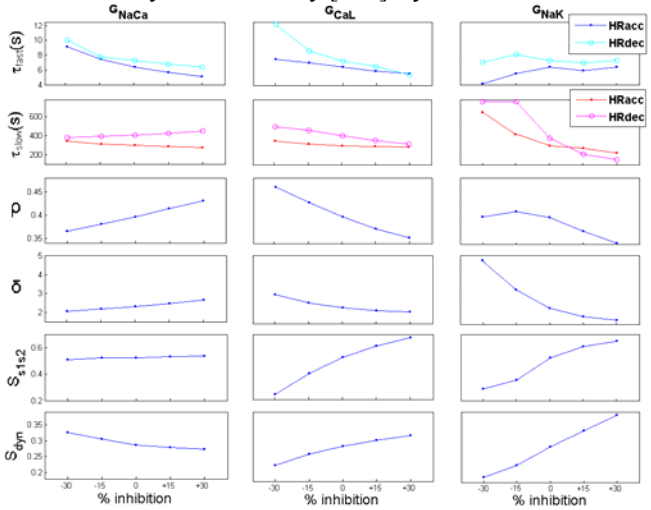

Figure 4. Relationship between APD adaptation time constants and arrhythmic risk markers (ρ, δ, S_{S1S2} and S_{dyn}) under variations from -30% to +30% in G_{NaCa}, G_{CaL}, and G_{NaK}.

3.4. Cardiac memory and arrhythmic risk

To study the relationship between increased CM and arrhythmic risk in atria, the electrophysiological markers ρ, δ, S_{S1S2} and S_{dyn} are examined under different simulated conditions known to alter APD adaptation dynamics.

Figure 4 shows that an increase in τ_{fast} caused by I_{NaCa} inhibition is not related to increased proarrhythmic risk, as quantified by any of the evaluated biomarkers. However, an increase in τ_{fast} induced by 30% I_{CaL} inhibition is associated with a more likely generation of afterdepolarizations, as assessed by higher probability of calcium reactivation (ρ close to 0.5), and AP triangulation (δ greater than 3). Under that simulated condition, both restitution slopes, S_{S1S2} and S_{dyn}, become substantially shallower (S_{S1S2} and S_{dyn} close to 0.2), which has been suggested to favor stability of reentry in some studies [5]. Additionally, Figure 4 shows that Na^+/K^+ pump inhibition contributes to delay the slow phase of APD rate adaptation and this is related to proarrhythmic risk, as indicated by a higher probability of calcium reactivation (ρ=0.4), larger AP triangulation (δ=4.7), and shallower APDR slopes (S_{S1S2}=0.3; S_{dyn}=0.2).

4. Discussion and conclusions

The present work focuses on investigating atrial APD response after sudden sustained changes in HR. To the best of our knowledge, this dynamic dependence has not been investigated in human atrium. There are some experimental studies in the literature analyzing CM in canine atrial tissue [1]. Due to lack of experimental human data, we have compared simulations in human with experiments in dog atria, and we have shown that APD rate adaptation is qualitatively similar, with the whole adaptation process taking some minutes to be completed and comprising fast and slow phases.

Furthermore, we have investigated how CM differs between atria and ventricles. We have found that the degree of CM is larger in atria, where time constants of fast and slow APD adaptation are: τ_{fast}=6.4/7.3 s, τ_{slow}=297.2/404.3 s following HR acceleration/ deceleration, while in ventricular epicardial cells they were found to be: τ_{fast}=10.8/22.0 s, τ_{slow}=128.3/120.9 s following HR acceleration/deceleration, as shown in [2]. Ionic mechanisms of CM are similar in the two cavities with regards to the slow adaptation phase, but not to the fast one, which can be explained by the different contribution of the involved ionic currents (I_{CaL}, I_{NaCa}, I_{Ks}) in atrium and ventricle.

Finally, one of the main objectives of the present study was to establish a relationship between CM in human atria and proarrhythmic risk. We have shown that a delayed APD rate response is associated with increased proarrhythmic risk due to either a higher probability of developing afterdepolarizations or to favoring stability of reentrant waves. Our results are in agreement with observations made in the experimental study reported in [1], where APD rate adaptation is evaluated in normal atria and in atria with induced atrial fibrillation, and it is shown that protracted adaptation is related to an increase in the probability of reactivating arrhythmias.

In conclusion, cardiac memory in human atria manifests in a slow APD adaptation following sudden sustained changes in HR; the adaptation process takes several minutes to be completed, and it is composed of two phases: a fast initial one involving the Na^+/Ca^{2+} exchanger and the L-type calcium current; and a second slow accommodation determined by intracellular Na dynamics. Delayed APD adaptation is found to be associated with increased proarrhythmic risk.

Acknowledgements

This study was supported financially by the European Commission preDiCT grant (DG-INFSO - 224381), an UK Medical Research Council Career Development Award (to B.R.), fellowship from Ministerio de Ciencia e Innovación, Spain (to E.P.), grant TEC-2007-68076-C02-02 from Ministerio de Ciencia e Innovación, Spain (to C.S., E.P. and P.L.), and fellowship BES-2008-002522 from Ministerio de Ciencia e Innovación, Spain (to C.S.).

References

[1] Hara M, Shvilkin A, Rosen MR, Danilo Jr P, Boyden PA. Steady-state and nonsteady-state action potentials in fibrillating canine atrium: abnormal rate adaptation and its possible mechanisms. Cardiovascular Research 1999;42:455-69.

[2] Pueyo E, Laguna P, Rodríguez B. Mechanisms of ventricular heart rate adaptation as an indicator of arrhythmic risk. Presented at Heart Rhythm Scientific Sessions, San Francisco, 2008.

[3] Courtemanche M, Ramirez RJ, Nattel S. Ionic mechanisms underlying human atrial action potential properties: insights from a mathematical model. Am J Physiol Heart Circ Physiol 1998;275:301-21.

[4] Narayan SM, Kazi D, Krummen DE, Rappel WJ. Repolarization and activation restitution near human pulmonary veins and atrial fibrillation initiation. Journal of the American College of Cardiology 2008;52(15):1222-30.

[5] Frame LH, Simpson MB. Oscillations of conduction, action potential duration, and refractoriness. A mechanism for spontaneous termination of reentrant tachycardias. Circulation 1988;78:1277-87.

[6] Viswanathan PC, Rudy Y. Pause induced early afterdepolarizations in the long QT syndrome: a simulation study. Cardiovascular Research 1999;42:530-42.

[7] Hondeghem LM, Carlsson L, Duker G. Instability and triangulation of the action potential predict serious proarrhythmia, but action potential duration prolongation is antiarrhythmic. Circulation 2001;103:2004-13.

[8] Nygren A, Fiset C, Firek L, Clark JW, Linblad DS, Clark RB, Giles WR. Mathematical model of an adult human atrial cell: the role of K^+ currents in repolarization. Circ Res 1998;82:63-81.

Address for correspondence: (Email: cstapia@unizar.es)

Carlos Sánchez, Department of Electronic Engineering and Communications, CPS, University of Zaragoza, Spain.